





ORIGINAL PAPER

Wild versus lab house mice: Effects of age, diet, and genetics on molar geometry and topography

Yoland Savriama¹  | Caroline Romestaing²  | Angéline Clair³ | Laetita Averty³ | Julie Ulmann³ | Ronan Ledevin⁴  | Sabrina Renaud⁵ 

¹Max-Planck Institute for Evolutionary Biology, Plön, Germany

²Laboratoire d'Écologie des Hydrosystèmes Naturels et Anthropisés (LEHNA), ENTPE, Université de Lyon, Université Claude Bernard Lyon 1, UMR 5023 CNRS, Villeurbanne, France

³Plateforme Animalerie Conventio nnelle et Sauvage Expérimentale de la Doua (ACSED), Fédération de Recherche 3728, Université de Lyon, Université Claude Bernard Lyon 1, CNRS, ENS-Lyon, INRAE, INSA, VetAgroSup, Villeurbanne, France

⁴PACEA, UMR 5199 CNRS, Université de Bordeaux, Pessac, France

⁵Laboratoire de Biométrie et Biologie Evolutive, UMR 5558, CNRS, Université Claude Bernard Lyon 1, Université de Lyon, Villeurbanne, France

Correspondence

Sabrina Renaud, Laboratoire de Biométrie et Biologie Evolutive, UMR 5558 CNRS, Université Claude Bernard Lyon 1, Université de Lyon, Campus de la Doua, 69100 Villeurbanne, France.
Email: Sabrina.Renaud@univ-lyon1.fr

Funding information

Fédération de Recherche BioEnviS, Grant/Award Number: FR3728

Abstract

Molar morphology is shaped by phylogenetic history and adaptive processes related to food processing. Topographic parameters of the occlusal surface, such as sharpness and relief, can be especially informative regarding diet preferences of a species. The occlusal surface can however be deeply modified by wear throughout an animal's life, potentially obliterating other signals. Age being difficult to assess in wild populations, especially small rodents, experimental studies of wear through age in laboratory populations may constitute a powerful way to assess its impact on molar geometry and topography, and to validate descriptors of molar morphology that could mitigate this issue. Molar morphology was therefore quantified using 3D geometric morphometrics and topographic estimates in four groups of house mice: wild-trapped mice, lab-bred offspring of these wild mice, typical laboratory mice, and their hybrids. Three descriptors of the molar morphology were considered: the surface of the whole molar row, the surface of the first upper molar, and a truncated template of the first upper molar mimicking advanced wear. Increasing wear with age was demonstrated in the different groups, with a more pronounced effect in the wild-trapped population. The geometry of the molar row is not only modified by wear, but also by the relative position of the late developing molars on the jaw due to loading during mastication. As a consequence, the alignment of the molars is modified in wild mice, showing a qualitative difference between wild animals and their lab-bred offspring. Results obtained from the lab should thus be transferred with caution to the interpretation of differences in wild populations. Topographic estimates computed for the first upper molar seems to provide more stable parameters than those based on the whole molar row, because issues related to non-planar occlusal surface along the molar row are discarded. The truncated template was proven efficient in discarding the wear effect to focus on genetic differences, allowing an efficient characterization of the hybridization signature between wild and lab mice. Dominance of the wild phenotype for the first molar shape supports that the lab strain evolved in a context of relaxation of the selective pressures related to nutrition.

KEYWORDS

dental functional morphology, geometric morphometrics, hybridization, mastication, *Mus musculus domesticus*, occlusal relief

1 | INTRODUCTION

The evolution of the mammalian dental pattern participated to the successful radiation of the group, by allowing efficient occlusion in face of various diets, and hence ecological diversification (Grossnickle et al., 2019; Hunter & Jernvall, 1995). Mammalian teeth therefore bear both a phylogenetic and an ecological signal. Being indurated, they have a good potential of preservation in the fossil record, even for otherwise fragile small mammals, and constitute a precious source of information to understand the history of the most speciose order of mammals, the rodents, including phylogenetic relationships and migration history (López-Antoñanzas et al., 2019; Misonne, 1969) and inference of diet for extinct species (Firmat et al., 2010). The development of 3D imagery of teeth, by providing metrics of functional significance, such as sharpness and complexity, opened new insights into the adaptive relevance of geometric differences observed between taxa (Boyer, 2008; Winchester et al., 2014).

In teeth without permanent eruption, wear is the only factor modifying tooth geometry and functional properties after eruption, but it constitutes an important source of variation which can vary depending on the diet (Renaud & Ledevin, 2017) and even be adaptive through the process of molar sculpting (Pampush et al., 2018). Yet, wear can be problematic because it can obliterate all other signals, including genetic differences in tooth shape (Ledevin et al., 2016; Pallares et al., 2017). The importance of wear signature on geometric and topographic tooth properties remain however largely unexplored, but may be important for the interpretation of differences between taxa (Pampush, Spradley, et al., 2016), and even more of differences between populations within a single species.

Assessing the effect of wear is challenging because it is dependent both on food consistency and on age, which is difficult to estimate in wild animals, especially for small mammals. Working on laboratory models may be relevant to provide standardized conditions of breeding and controlled ages, allowing a precise characterization of wear patterns as a function of age and diet (Renaud & Ledevin, 2017). It remains to be addressed, however, if wear patterns observed in standard laboratory conditions are comparable to those observed in wild populations. Two effects may be involved. First, most laboratory strains originated ~100 years ago (Wade et al., 2002), a time long enough for evolution to occur, both due to drift in restricted populations and due to adaptation to the very special conditions of lab breeding, including food ad libitum. Laboratory strains may thus be inadequate models for understanding mastication and its effect in the wild. Furthermore, the mere translocation of wild animals to lab conditions will change many aspects of their environment, including the quality and accessibility of food resources, possibly changing wear trajectories compared to wild conditions.

The aim of the present study is thus to quantify molar shape and topography in a set of house mice (*Mus musculus domesticus*), documenting a classical laboratory strain, a wild population, and the effect of translocation to laboratory conditions. The relative importance of genetically driven morphological changes, and of all those

occurring, primarily due to wear, as the teeth are being used (later on designed as “use-related” changes), may depend on the geometric descriptors of the molars. Three approaches were therefore compared. The molar row, constituted of three teeth in murine rodents, may be considered as the functional unit in the chewing process, and thus the most adequate character to address functional issues (Renaud & Ledevin, 2017; Renaud et al., 2018). Alternatively, working on isolated molars facilitates an extrapolation to fossil material (Pampush et al., 2018; Winchester et al., 2014). Finally, wear-related changes may be discarded by focusing on unworn parts of the teeth, in order to focus on genetic differences (Ledevin et al., 2016; Pallares et al., 2017).

Four groups were therefore compared: (1) wild-trapped house mice, (2) offspring bred from this wild population in laboratory conditions, (3) typical outbred laboratory mice from the Swiss strain, and (4) hybrids between wild-derived offspring (group 2) and Swiss (group 3). For all mice, the geometry and topography of the upper molar row, of the first upper molar, and of its truncated model, were quantified and compared. The upper row, and within it the first molar, were selected because they are more evolvable than their lower counterpart in house mice (Hayden et al., 2020; Renaud et al., 2011).

Hypotheses to be investigated were the following. (1) Rearing mice in laboratory conditions should affect use-related trajectory, even in mice sharing the same genetic background. (2) Laboratory strain should exhibit morphological differences compared with wild mice, due to their long history of evolution in isolation. (3) Neutral divergence due to drift and relaxation of adaptive pressure related to feeding behavior should lead to different patterns of hybridization. Neutral divergence, due to the accumulation of mutations in the two parental conditions, should lead to intermediate hybrids. By contrast, relaxation of selection may lead to the accumulation of unfavorable, recessive alleles in the lab strains, leading to a dominance of the wild phenotype in hybrids. (4) Regarding the descriptors of molar geometry, use-related effect should be the most important when considering the molar row as a whole, whereas genetic differences should be best described when focusing on unworn parts of the teeth.

2 | MATERIAL

Western European house mice (*M. m. domesticus*) were collected during two trapping campaigns in a horse stable in Balan, nearby Lyon, France (45°49'09"N, 5°05'41"E). All mice were killed at capture in 2015. In 2017, two mice were killed at capture and 31 animals were brought to the animal facility (ACSED, Lyon University). After approximately 2 months of acclimation, they were paired to obtain offspring that were bred with standard rodent pellets (SAFE A04), with food and water ad libitum.

Adult Swiss mice (Hsd:ICR [CD-1®]) were bought from Envigo. This strain was chosen because among classical laboratory strains, it is phylogenetically the closest to *M. m. domesticus* (Yang et al., 2011). Two mixed pairs were formed, composed of one male Swiss with a F1 female, and another of one female Swiss with a F1 male, to

deliver hybrid descendants that were bred in the same conditions as offspring of wild-trapped mice.

Breeding was conducted in accordance with animal care guidelines in an accredited animal facility. The mice were killed according to the directive 2010/63/UE of the European Parliament on the protection of animals used for scientific purposes.

2.1 | Material for the 3D morphometric analysis

The sampling for the 3D study included 30 mice ranging from 3 weeks to almost 4 months of age (Table S1). Seven wild-trapped mice from Balan were included, together with 14 laboratory offspring. Five Swiss mice were also measured, as well as four hybrids issued from crosses between Swiss and Balan F1 mice. Sex has been demonstrated to have little effect on molar size and shape in house mice (Renaud, Hardouin, et al., 2017; Valenzuela-Lamas et al., 2011). Males and females were therefore pooled in the analysis. One young mouse at weaning (21 days of age) was included in the analysis. However, since its third molar was on the course of eruption, it did not display a continuous and fully grown molar row. This prevented its inclusion in the analysis of the molar row, but it was included in the analysis of the first upper molar as a reference of unworn tooth geometry.

3 | METHODS

3.1 | Acquisition and extraction of 3D surfaces

Skulls were scanned at a cubic voxel resolution of 12 μm (except for SW01 and SW02 scanned at 13.5 μm) using a Phoenix Nanotom S microtomograph (μCT) on the AniRA-ImmOs platform

of the SFR Biosciences, Ecole Normale Supérieure. For each mouse, the right upper molar row (UMR) was delimited using Avizo (v. 9.1—Visualization Science Group, FEI Company). In most cases, an automatic threshold was sufficient to isolate the molar row from the surrounding bone and generate a surface including the roots; in a few cases, connections with the bone had to be manually delimited. The first upper molar (UM1) was also delimited. Due to its contact with the second molar, it had to be manually isolated, starting from the volume extracted for the complete upper molar row.

3.2 | 3D description

Mouse molars are composed of transverse enamel ridges (Figure 1), the cusps of which align to form longitudinal rows that guide the propalinal (antero-posterior) movement during chewing. The molar row has a complex and variable geometry that prevents to reliably locate landmarks and delineate curves along the ridges. The ridges are delineated by a contact between enamel and dentine; therefore, the dentine surface is also affected by wear, preventing the use of the dentine surface as a wear-free descriptor of the tooth geometry (Skinner & Gunz, 2010). Therefore, the molar morphology was described using surfacic templates describing the erupted part of the teeth and removing the roots (Ledevin et al., 2016; Renaud & Ledevin, 2017).

A specimen of intermediate age (Balan Lab #86) was selected for designing templates specific to the dataset (Figure 1). Three template surfaces were designed, describing (1) the upper molar row, with the three molars in contact (UMR); (2) the first upper molar (UM1) and (3) the truncated UM1 (UM1tr; Figure 1). This latter template was considered because the effect of wear on tooth shape can be a major cause of shape variation (Pallares et al., 2017; Renaud & Ledevin, 2017;

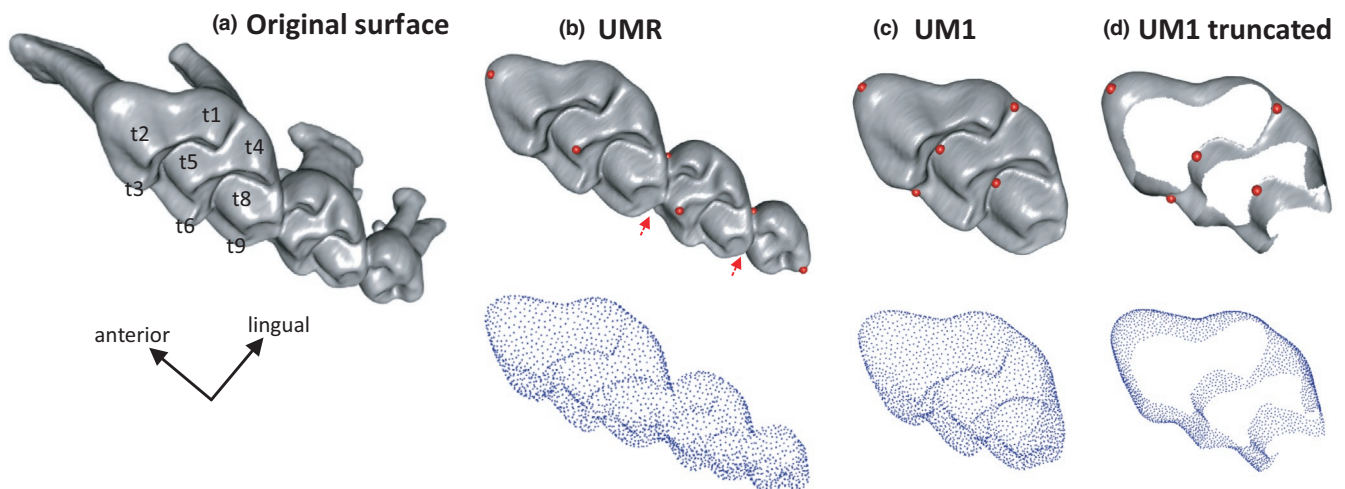


FIGURE 1 Descriptors of the mouse upper molars used in the morphometric study. (a) Original surface of the molar row, including the roots. (b–d, above) Templates describing the erupted part of the molar row (b), of the first upper molar (c) and truncated template mimicking wear (d). The red dots indicate the fixed landmarks used for the pre-orientation of the template; the red arrows point to hidden landmarks. The templates have been prepared on the specimen Balan Lab #86. (b–d, below) Set of semi-landmarks describing the surfaces

Renaud et al., 2018). By designing a truncated template with the top of the cusps cut to mimic an advanced degree of wear, the effect of the degree of tooth abrasion on the morphological signal can be mitigated (Ledevin et al., 2016; Pallares et al., 2017). The height at which the template was cut was decided empirically, assuring that the most worn teeth in the dataset were still adequately described with the template. The area of contact between the first and second molars was also removed to discard the impact of manual error during segmentation. This template will be referred as “truncated” or “wear-free.” A truncated template was not designed for the upper molar row, because mechanical loading associated with mastication seems to even impact the alignment of the three molars (Renaud & Ledevin, 2017). Such an effect could not be removed using a truncated template.

The templates were used to extract new surfaces limited to the zone of interest in the molar row. Fixed landmark were manually collected on all original surfaces using IDAV Landmark Editor v.3.6 (Wiley et al., 2005) in order to guide the application of the template on each of these surfaces. Eight landmarks were collected on the molar row for anchoring the UMR template (Figure 1): two on the UM1, one on the UM2, one on the UM3, and two at each junction between molars (UM1/UM2 and UM2/UM3). This was deemed sufficient to orient the structure according to anterior-posterior and lateral directions and allow the positioning of the template on each surface. When focusing on the first molar, the two previous UM1 landmarks were complemented by three additional landmarks which were located in valleys between the ridges or laterally relatively low on the crown, so that they could be used for both UM1 and UM1tr. These fixed landmarks were used as priors to guide the registration process of equally spaced sliding semi-landmarks on the new surfaces using the package Rvcg (Schlager, 2017). The number of semi-landmarks was automatically selected during the procedure, leading to 2186 landmarks for the UMR, 2199 for the UM1, and 2293 for the truncated UM1 (Figure 1).

Furthermore, in order to retrieve a proxy of body size, the length of the mandible was extracted for each mouse from two points located on a 3D isosurfacic model at the anteriormost point of the mandibular bone along the incisor, and the posterior extremity of the condyle. This measure was selected because mandible size has been shown to display very little sexual dimorphism and to be well correlated to body size (head + body length; Renaud, Hardouin, et al., 2017).

3.3 | Geometric morphometric analyses

The sliding procedure for surface semi-landmarks was done using minimum bending energy (Bookstein, 1997) via function `slider3d()` from the Morpho package (Schlager, 2017). A generalized Procrustes analysis was applied to the dataset including the semi-landmarks only. This superimposition extracted shape, described by aligned (Procrustes) coordinates, by removing extraneous effects of location, orientation, and position; it was carried out with function `procSym()` from Morpho. A principal component analysis (PCA) was applied to variance-covariance matrix of the Procrustes coordinates using the R

package `geomorph` (Adams & Otarola-Castillo, 2013) to extract the PC scores later used as shape data in subsequent analyses. Centroid size, the most common and explicit measure of size in geometric morphometrics, was computed as the square root of the sum of the squared distances of all landmarks from their centroid (Slice et al., 1996).

3.4 | Topographic analyses

The topographic parameters were computed from the surfaces of the upper molar row and of the first upper molar used for the geometric morphometric assessment of their shape. The templates were used to discard the root portions of the original surface that would otherwise cause errors during computation of the complexity parameters.

Topographic calculations require that the occlusal surface of each tooth row is aligned with the X and Y planes, lying face-up, and oriented orthogonal to the Z-axis. First, the occlusal surface of the template dental row was manually oriented according to the aforementioned standardization using the “Align” module in MeshLab (Cignoni et al., 2008). Second, the `icp()` function from the `mesheR` package (Schlager, 2015) was used for pairwise automatic surface registration of each tooth row onto the standardized dental template using first the fixed landmarks for global registration followed by a series of iterations using the Iterative Closest Point family of algorithms (Besl & McKay, 1992) to further refine the registration process. Third, all surfaces were simplified to 10,000 faces (Pampush, Winchester, et al., 2016) using function `vcgQDecim()` from `Rvcg` package (Schlager, 2017).

Four parameters were used to characterize the topographic properties of the molar rows. Dirichlet normal energy (DNE) assesses tooth sharpness by measuring the curvature and undulation of the surface (Bunn et al., 2011). Orientation patch count (OPC) estimates the number of separately oriented facets on a tooth surface and is considered a proxy for dental complexity (Evans et al., 2007). It is measured by dividing a tooth surface into contiguous patches that share an orientation and then summing the number of such patches. The Orientation Patch Count Rotated (OPCR) averages OPC estimates obtained by rotating the surface from its original orientation by 5.625° a total of eight times around the Z-axis (Evans & Jernvall, 2009). Relief Index (RFI) corresponds to the log ratio between the surface area of a tooth's crown (Area3D) and the area of the tooth planometric footprint (Area2D; Boyer, 2008). Finally, slope corresponds to the average slope of the occlusal surface (Zuccotti et al., 1998).

The 3D surfaces of the UMR, UM1, and UM1tr have been deposited in MorphoMuseum (Renaud et al., 2021). Data about the scanned specimens, centroid size, PC scores, and topographic parameters can be found in Table S1.

3.5 | Statistical analyses

Differences in univariate parameters (size estimates and topographic parameters) between the four groups (Balan W, Balan L, Hybrids and

Swiss) were tested using non-parametric Kruskal–Wallis tests complemented by pairwise Wilcoxon tests.

Next, statistical analyses were performed on various subsets of specimens in order to test the different hypotheses. (1) A first analysis tested the effect of breeding conditions on wear trajectories. Wild-trapped mice (Balan W) and their laboratory offspring (Balan L) were included in these analyses. The variations of molar geometry and topography were investigated as a function of different proxies for life stage (weight, age, and/or mandible length) depending on the group(s) considered. (2) A second analysis investigated the differences between laboratory strain (Swiss) and wild-derived mice (Balan L). Differences in molar geometry were tested using multivariate analyses of variance using the package *ffmanova* (Langsrud & Mevik, 2012). Differences in size and topographic parameters were tested using *t*-tests that perform well even with very small sample sizes (de Winter, 2013). Differences in age-related trajectories were tested using linear models. (3) A third analysis focused on hybridization between Balan L and Swiss mice (groups involved: Balan L, Swiss, and hybrids).

In order to characterize the position of the hybrids between parental groups, between-group PCA were performed, based either on all PC axes, or on the first three PCs only, for the UMR, the UM1 and the truncated UM1, using the package *ade4* (Thioulouse et al., 2018). Hybrids were further characterized by dominance and transgressivity indices calculated from PC scores describing molar geometry. The degree of transgression was assessed as the deviation of the hybrids from the theoretical expectations of them being along the range of possible intermediates between parents, hence $d[(\text{Hybrids}, \text{Balan L}) + d(\text{Hybrids}, \text{Swiss}) - d(\text{Balan L}, \text{Swiss})]$, expressed as a percentage of the inter-parental strains distance $d(\text{Balan L}, \text{Swiss})$ (Renaud et al., 2012). The degree of closeness to a parental strain, pointing to dominance-like pattern, was estimated by assessing the difference in the distance to one parental strain (here, Balan L taken as reference) with respect to the average distance between the hybrids and the two parental groups, hence $d[(\text{Hybrids}, \text{Balan L}) + d(\text{Hybrids}, \text{Swiss})]/2 - d(\text{Hybrids}, \text{Balan L})]$, expressed as the percentage of the average distance of hybrids to the parental strains $d[(\text{Hybrids}, \text{Balan L}) + d(\text{Hybrids}, \text{Swiss})]/2]$ (Renaud et al., 2012). Positive values then indicate closeness to Balan L, and negative values closeness to the Swiss parental group. The distances were estimated on the PCs based on the aligned coordinates. A first series of estimates was based on a reduced data set, focusing on the axes totaling most morphological variance (first three PCs). A second series of estimates was based on all PCs.

All analyses were performed under R (R Core Team, 2018).

4 | RESULTS

4.1 | Body, mandible, and molar size

Three possible indices to trace the signature of advancing use on tooth geometry were investigated: age, body weight, and mandible size. Age was known for lab-reared animals but not for wild-trapped mice. Body weight was available for most mice, including

wild-trapped mice. However, it can be affected by body size but also by health status and sex. Furthermore, it differs between the wild line and the much larger Swiss strain (mean weight Balan W = 14.4 g; Balan L = 18.9 g; Swiss = 39.5 g). Since weight is presumably more related to volume than to linear size, its cubic root was considered in the analyses. Increasing weight with age was demonstrated within Balan L ($R = 0.7162$, $p = 0.0059$), the only group with a satisfying sample size ($N = 13$) for these variables.

Mandible size was further investigated as a proxy of body size, available for all mice. Mandible length was significantly related to body weight across the dataset including the four groups (Balan W, Balan L, Swiss, Hybrid); $R = 0.8902$, $p < 0.0001$). When considering group and sex as co-factors (Mandible Length ~ Weight^{1/3} + Group + Sex), mandible length was still related to weight ($p = 3.521e-08$) but not to group ($p = 0.5478$) or sex ($p = 0.8382$).

The centroid size of the upper molar row increased with mandible size ($R = 0.5929$, $p = 0.0007$) (Figure 2A). Swiss and hybrids mice displayed larger molar rows than Balan mice (Figure 2B; Table 1) in agreement with their larger mandible and body size. By contrast, the relationship was not significant when considering the UM1 ($R = 0.1951$, $p = 0.3016$) and the truncated UM1 ($R = 0.1653$, $p = 0.3826$). The four groups displayed similar UM1 and UM1tr centroid size (Table 1). Wild mice displayed a large variation in molar centroid size (Figure 2B–D). UM1 centroid size was even negatively related to mandible size in this group (Balan W: $R = -0.7656$, $p = 0.0448$), suggesting that this variation was related to the abrasion of the cusps increasing with age.

4.2 | Geometric and topographic differences between the four groups

4.2.1 | Pattern of shape differences

When considering the upper molar row (Figure 3A,B), the first order signal was an important variation within wild-trapped mice along PC1 (30.4% of variance). This axis describes an increasing abrasion of the cusps toward positive scores, but also a change in the relative arrangement of the three molars. Whereas the molars are well aligned in unworn rows (negative scores), the UM1 becomes oblique relative to the UM2 and UM3 in rows characterized by advanced wear (positive scores). All laboratory-reared mice (Balan L, Swiss, Hybrids) appear clustered along PC1, toward low scores and hence low degree of wear and aligned UM1–UM2–UM3. Between-group differences are expressed along PC2 (17.7%) and PC3 (9.2%). Balan laboratory offspring differ from their wild relatives along PC2, especially due to the third molar (UM3) aligned with the two other molars in laboratory-bred mice while the UM3 is shifted toward the lingual side in wild-trapped mice. PC2 also differentiates four out of five Swiss mice from the wild mice and the hybrids. The difference between Swiss and wild mice is mostly expressed along PC3 (Figure 3B), corresponding to a more elongated and lingually deflected anterior part of the first upper molar, and a labially expanded

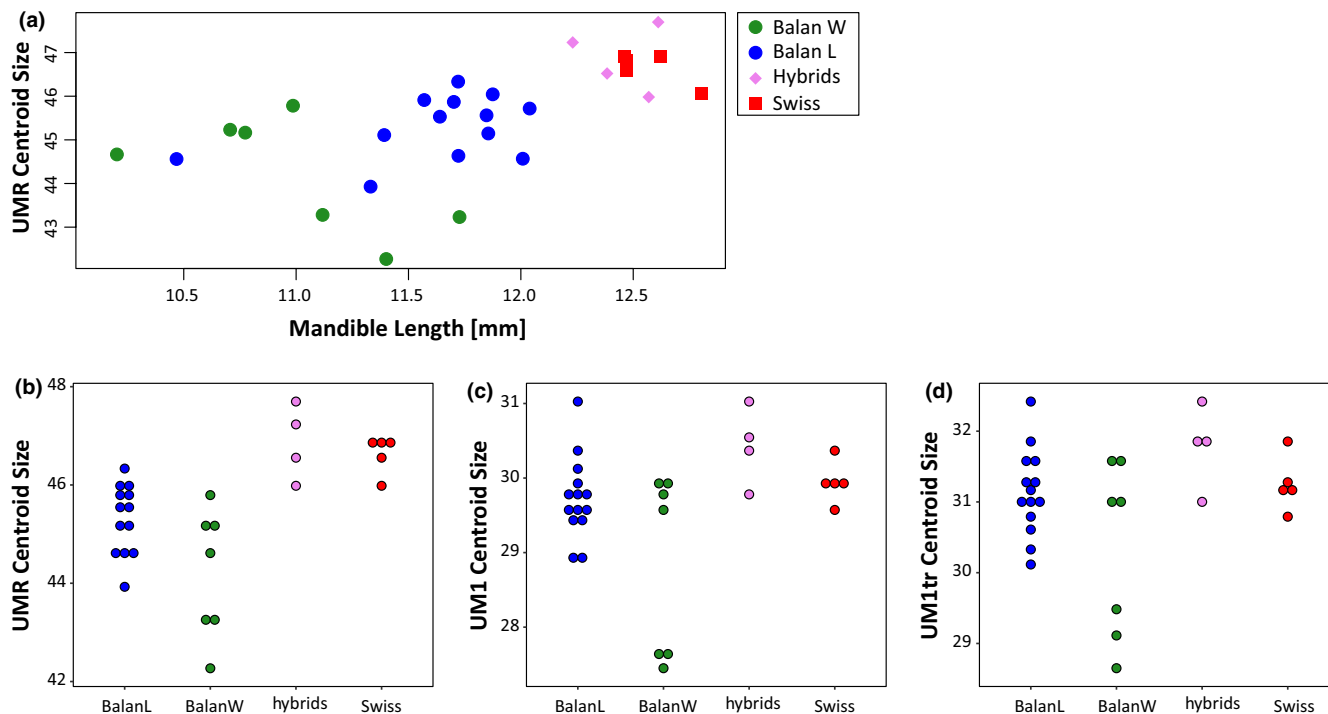


FIGURE 2 Centroid size of the upper molar row (UMR), and of the first upper molar (UM1). (a) UMR centroid size as a function of mandible length, as a proxy of body size. (b–d) Centroid size in the four groups, for the molar row (b), the first upper molar (c) and the truncated first upper molar (d)

TABLE 1 Differences in centroid size between groups. The p -values of Kruskal–Wallis (KW) are provided, followed by p -values of pairwise post-hoc Wilcoxon tests. In bold: $p < 0.001$; underlined: $p < 0.01$; in italics: $p < 0.05$

	KW	BW-BL	BW-Hyb	BW-SW	BL-Hyb	BL-SW	Hyb-Sw
UMR	0.0004	0.2293	0.0134	<u>0.0028</u>	0.0182	0.0126	0.9048
UM1	0.0485	0.60	0.17	0.60	0.15	0.60	0.60
UM1tr	0.1024	1.00	0.31	1.00	0.15	1.00	1.00

t5 cusp in Swiss mice. Hybrids plot with the Swiss parental group along PC3 but with the Balan parental group along PC2.

Focusing on the first upper molar (UM1; Figure 3C), the first PC (41.9%) also describes an increasing abrasion of the cusp; wild-trapped mice are very variable along this axis. Differences between groups are expressed along PC2 (11.7%), with Balan L and Balan W sharing a similar range of variation, Swiss mice being well differentiated and hybrids plotting close to the Balan parental group.

When considering the truncated template of the first upper molar (UM1tr; Figure 3D), the difference between groups is expressed on the first axis (PC1 = 22.1%). Swiss mice are well differentiated while hybrids plot close to the Balan parental group. Lab and wild Balan mice share a similar range of variation in the morphospace.

4.2.2 | Topographic parameters

Since these parameters describe the topography of the surface, they appeared to be meaningless on the truncated template. Therefore,

only descriptors that include the occlusal surfaces (UMR and UM1) were used (Figure 4). Values obtained from the UMR and the UM1 display similar trends, with less variation when focusing on the UM1, especially for RFI and OPCR. Laboratory-reared mice (Balan L, Hybrids, Swiss) display overall a moderate variance and their values overlap. Wild-trapped mice (Balan W) exhibit a much larger variation for all parameters, with values exceeding the range observed for laboratory-bred mice.

4.3 | Differences along life history: Wild-trapped mice versus lab offspring

In order to assess the impact of acclimation to laboratory conditions, the next analyses focused on the comparison of wild-trapped mice (Balan W) and their lab-bred offspring (Balan L). Shape variations were first considered, taking scores on PC1 as estimates of the most important shape changes. The impact of life history was assessed by comparing shape to the available proxies for life stage: weight

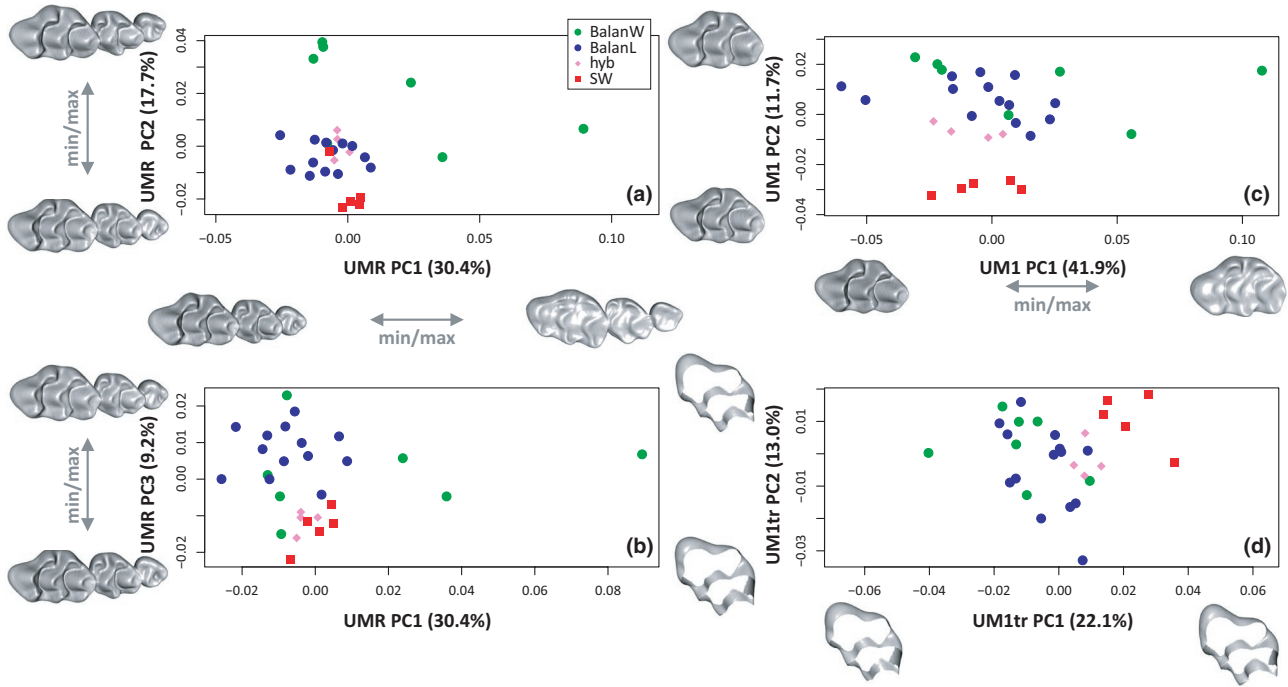


FIGURE 3 Shape differentiation of the molars. (a, b) Upper molar row. (c) First upper molar. (d) Truncated template of the first upper molar. (a, c, d) Second versus first axis of a principal component analysis (PCA) on the aligned coordinates. (b) Third versus first axis of the PCA depicted in A. Shapes corresponding to extreme scores along the axes are represented along each axis

and mandible size for Balan W, and age, weight and mandible size for Balan L (Table 2). Shape (PC1) was related to life stage for the UMR and the UM1, but this could only be shown using age and to a lesser degree, weight. UM1tr shape was not related to any proxy of life stage (Table 2).

Models including weight, group, and interaction as factors were further considered (Table 3). For both the UMR and UM1, the three effects were significant, showing that shape varied in both groups according to life stage, but with different slopes (Figure 5). Shape changes occurring with increasing weight were indeed much more pronounced in Balan W than in Balan L. No significant variation occurred when considering the shape of truncated UM1, confirming that wear effect was efficiently discarded. Swiss mice, which were not included in the previous linear models, display UMR and UM1 shape scores in the range of those observed in Balan L. This was further tested by models assessing the variations along PC1 in Balan L and Swiss mice as a function of age and population (Table 3). The effect of age was significant but not the population effect nor the interaction term, showing that in lab conditions, both genetic lines shared similar trajectories.

When considering Balan W and Balan L, the four topographic parameters appeared to vary throughout the lifespan. Most significant results were obtained for the UM1 alone. The variation in the alignment of the three molars may have rendered the orientation of the occlusal surface too variable for estimating comparable topographic parameters. Relief (RFI) was the most impacted by changes along life, with significant variations for the UMR and the UM1 (Table 3). Related to abrasion, this signal was most pronounced in

wild-trapped mice (Figure 6). Molar slope tended to decrease along life, as expected with an abrasion of cusp tips. This effect was much more pronounced in wild-trapped mice UM1. Decrease in sharpness (DNE) was less obvious, although marginally significant for the UM1 of wild-trapped mice. By contrast, complexity (OPCR) tended to increase along life, and this effect was similar in wild-trapped and lab-born animals.

4.4 | Differences between wild and laboratory strains, and their hybridization

Differences between wild-trapped and lab-bred Balan mice mostly involve the top of the cusps, and the torsion of the molar row occurring in old animals. These differences seem to increase along life as a response to functioning. By contrast, differences between Balan and Swiss mice involves the position and size of several cusps, with the most prominent changes apparent on the UM1 (Figure 7) whereas the trajectory of geometric change along life is similar in the two genetic lines (Table 3). Compared with Balan mice, Swiss mice are characterized by a reduced anterior lingual cusp (t2), an expanded posterior labial cusp (t9) and a central cusp (t5) extended labially. These geometric differences are significant considering the UMR, UM1, and truncated UM1 (Table 4). They have consequences on topographic parameters. The UM1 differed in sharpness, relief, complexity, and slope between the two groups, being higher in Swiss mice compared with Balan L (Table 4; Figure 4). The strongest effect is observed for complexity, which also differs

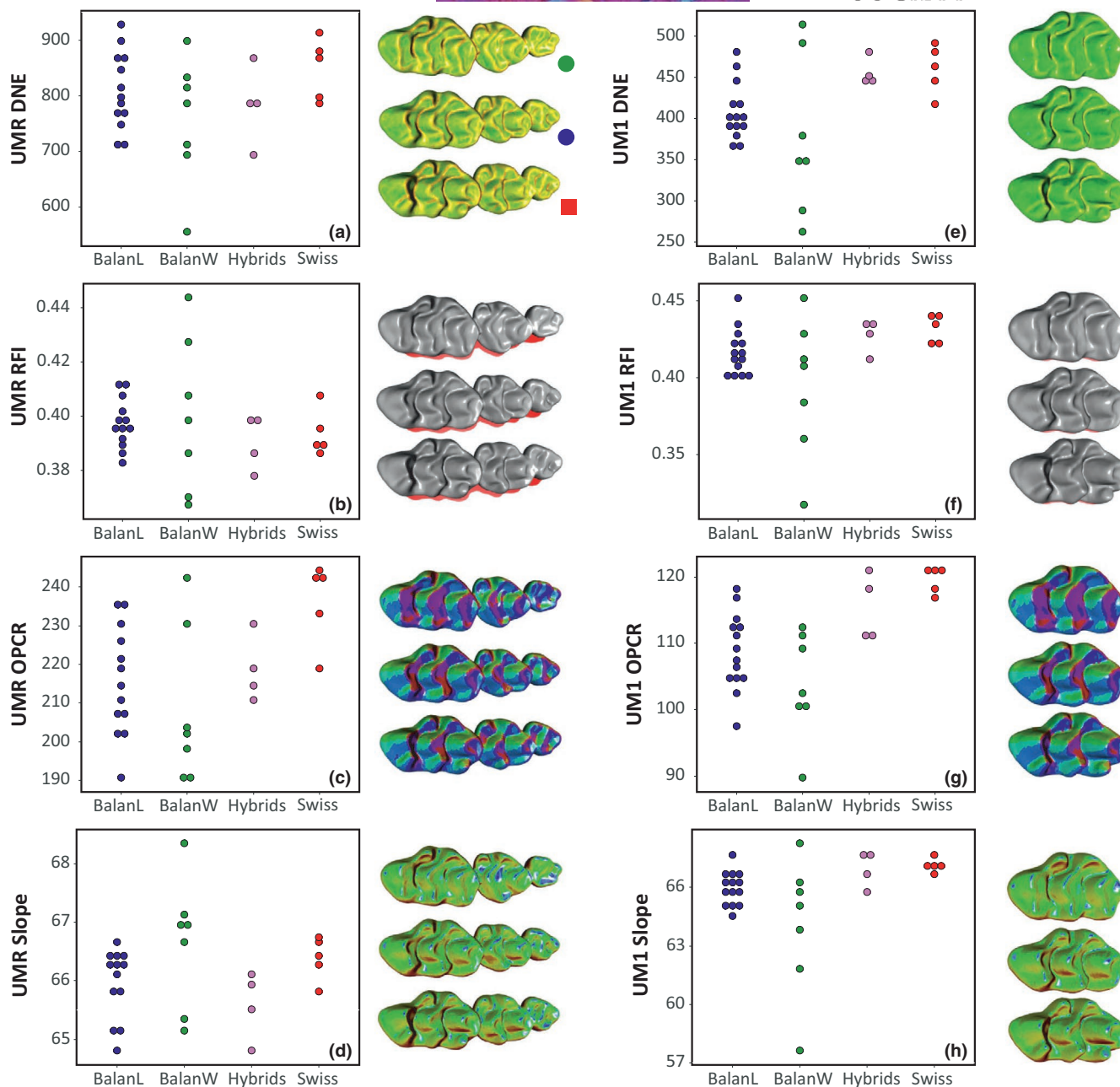


FIGURE 4 Topographic parameters estimated in the four groups for upper molar row (a–d) and the first upper molar (e–h). (a, e) tooth curvature (DNE, Dirichlet Normal Energy). (b, f) tooth relief (RFI, Relief Index). (c, g) tooth complexity (OPCR, Orientation Patch Count Rotated). (d, h) tooth slope. Next to each graph, visual representation of the variation of the topographic parameter on examples of the three main groups. Balan Wild #08 (17.3 g); Balan Lab #86 (template; 108 days, 24 g); Swiss #343 (74 days, 37.5 g). Scale of DNE and Slope: cold to warm color = low to high values; the three representations of a given panel at the same scale

when considering the complete molar row (UMR). An effect of age was further documented for relief only (Table 3), but these results should be considered with caution due to reduced sample size for the Swiss group.

The position of the hybrids relative to both parental groups varied depending on the character and the variable considered (Figure 8). When considering the total shape variation (all PC axes), hybrids displayed a transgressive morphology for the UMR, the UM1, and the truncated UM1. An example of this transgressive pattern is shown

by the labial cusp t4, which decreases from Balan to hybrids, but increases from hybrids to Swiss, hence showing little differences between the parental groups (Figure 7). When focusing on the most prominent geometric signal, summarized on the first three PC axes, transgression faded away for the UM1 and the truncated UM1 (Figure 8E,F). Dominance was low for the UMR, but was important when considering the UM1, being truncated or not. Always in favor of the Balan L parental group, it reached 25% when focusing on the first three PC axes.

TABLE 2 Relationship between shape, topographic parameters, and life stage. Shape is represented by scores on PC1 for the UMR, UM1, and UM1tr. Estimates of life stage are age, cubic root of weight, and mandible length (MdL). Coefficient of correlation and *p*-value of a Pearson's product-moment correlation computed within Balan W or within Balan L are provided. In bold: $p < 0.001$; underlined: $p < 0.01$; in italics: $p < 0.05$

Shape	PC1 vs.	UMR		UM1		UM1tr	
		R	<i>p</i> -value	R	<i>p</i> -value	R	<i>p</i> -value
Balan W							
PC1	Weight ^{1/3}	0.9542	0.0008	0.9250	<u>0.0028</u>	0.0794	0.8656
PC1	MdL	0.7047	0.0770	0.7658	0.0448	-0.0130	0.9779
Balan L							
PC1	Age	0.7168	<u>0.0058</u>	0.8211	0.0003	-0.2187	0.4524
PC1	Weight ^{1/3}	0.2387	0.4549	0.6871	<u>0.0095</u>	-0.0181	0.9532
PC1	MdL	-0.2645	0.3824	0.4319	0.1230	-0.0887	0.7630
Topography							
Balan W							
DNE	Weight ^{1/3}	-0.1226	0.7934	-0.7132	0.0720		
RFI	Weight ^{1/3}	-0.7674	0.0440	-0.8826	<u>0.0085</u>		
OPCR	Weight ^{1/3}	0.7265	0.0644	0.1541	0.7415		
Slope	Weight ^{1/3}	-0.0886	0.8502	-0.8771	<u>0.0095</u>		
Balan L							
DNE	Weight ^{1/3}	0.4418	0.1504	-0.1579	0.6064		
RFI	Weight ^{1/3}	-0.3452	0.2718	-0.4290	0.1435		
OPCR	Weight ^{1/3}	0.5385	0.0709	0.6476	0.0167		
Slope	Weight ^{1/3}	-0.7062	0.0103	-0.3902	0.1874		
Balan L							
DNE	Age	-0.4389	0.1335	-0.4020	0.1542		
RFI	Age	-0.6788	0.0107	-0.6407	0.0136		
OPCR	Age	-0.0475	0.8775	0.3887	0.1696		
Slope	Age	-0.5690	0.0424	-0.5192	0.0571		

5 | DISCUSSION

5.1 | Different molar descriptors highlight different sources of morphological variation

The murine dental formula is reduced, with no premolar and three molars only. Designing adequate template is a way to capture the geometry of the whole molar row as a functional unit to focus on the first upper molar, or on a truncated model discarding parts first eroded by wear. Our results confirmed that the descriptors including the occlusal surface were heavily impacted by wear but that considering the truncated model mimicking wear discards this effect and pinpoints genetic differences in tooth shape for genome-wide mapping (Pallares et al., 2017) or for retrieving phylogenetic information from wild-trapped populations for which age is not controlled (Ledevin et al., 2016). In the present case, the truncated model put the focus on genetic differences between wild mice and the laboratory strain. Despite the large parts of the molar surface that are not included in the description of the tooth, such a template proves to be efficient in describing the relative position and extension of the

cusps, and therefore retains most geometric information relevant to morphological differences with a genetic basis. However, the geometric information being retained is mostly located around the tooth. Compared with such truncated descriptor, 2D analysis of the molar outline may represent a moderate simplification, while allowing for a more extensive sampling than 3D analyses (Ledevin et al., 2016).

By contrast, the templates including the occlusal surfaces were both heavily impacted by variation occurring with use. For both the first upper molar and the upper molar row, abrasion of the cusps was an obvious effect of primary importance. Considering the molar row further showed that the relative arrangement of the three molars was modified as well. The alteration of the initial molar alignment suggests that the insertion of the molars changed on the jaw due to bone remodeling as a response to the functional constraints of occlusion. Probably due to these rearrangements, topographic parameters evaluating functional performance of the teeth appeared to be less stable and informative considering the molar row than focusing on the first upper molar.

Therefore, the different templates highlight different aspects of molar geometry. The truncated first upper molar reveals heritable

TABLE 3 Effect of life stage, breeding conditions, and genetic line on shape and topographic parameters. Two comparisons are presented: Balan W/Balan L (life stage estimated by the cubic root of weight) and Balan L/Swiss (life stage directly provided by age). The models include life stage, group and interaction (W:G or Age:G) on shape (estimated by scores on PC1) and topographic parameters. *p*-values of linear models are provided for the analysis of the upper molar row (UMR) and the first upper molar (UM1). In bold: $p < 0.001$; underlined: $p < 0.01$; in italics: $p < 0.05$

	Groups	UMR			UM1		
		Weight ^{1/3}	Group	W:G	Weight ^{1/3}	Group	W:G
Balan W vs. Balan L	Shape (PC1)	0.0243	2.190e-06	4.292e-05	0.0006	0.0003	0.0024
Balan W vs. Balan L	DNE	0.2713	0.5704	0.2989	0.2270	0.0387	0.0231
Balan W vs. Balan L	RFI	<u>0.0087</u>	0.1592	0.0292	0.0204	0.0008	<u>0.0011</u>
Balan W vs. Balan L	OPCR	<u>0.0056</u>	0.3311	0.5738	0.0197	0.5625	0.4440
Balan W vs. Balan L	Slope	0.0323	0.5365	0.3175	0.0396	0.0002	0.0005
		Age	Group	Age:G	Age	Group	Age:G
Balan L vs. Swiss	Shape (PC1)	0.0050	0.1000	0.0939	0.0003	0.3855	0.1736
Balan L vs. Swiss	DNE	0.0679	0.1696	0.9086	0.2324	0.0035	0.8476
Balan L vs. Swiss	RFI	0.0029	0.4894	0.8524	0.0314	0.0059	0.4509
Balan L vs. Swiss	OPCR	0.6832	0.0089	0.4003	0.0761	0.0016	0.2266
Balan L vs. Swiss	Slope	0.0678	0.0911	0.3339	0.1794	0.0074	0.2413

differences by discarding wear effects. Considering the complete molar row may provide best insights into functional constraints, because it will not only capture the signature of cusp abrasion but also of tooth rearrangement related to functional loadings during mastication. Finally, considering an isolated molar (here the first upper one) provides geometric description still heavily influenced by wear, but efficiently estimates of topographic parameters to get insight into the tooth response to diet.

5.2 | Use-related trajectories, tracers of breeding conditions

The comparison of wild-trapped and lab-bred mice showed that use-related changes were very important on the molar morphology, and that they depended on the breeding conditions. Changes of tooth geometry along life were demonstrated in all well-documented groups: wild-trapped mice and their laboratory offspring, and Swiss mice. Laboratory-bred animals, being wild-derived or from the Swiss strain, shared a similar trajectory of molar shape change along life. By contrast, wild-trapped animals displayed a different trajectory leading to more advanced wear for the same estimated life stage. These results show that wear trajectories through the animals' life, and more generally the signature of use on the molar row, can differ dramatically in response to diet. Differences in tooth row geometry have been documented between laboratory mice fed hard versus soft food (Ledevin et al., 2016). In that case, differences in wear trajectory due to diet were not as pronounced as here, possibly as the results of limited wear in laboratory mice compared with situations in the wild. The steeper wear trajectory in wild mice shows that the functional demand related to occlusion was much weaker in laboratory mice fed regular rodent pellets than in mice which, trapped in a stable, had access to straw, hay, and rests of flaked cereals. Either rodent pellets are easier

to disintegrate with the sole action of the incisors, and/or mice fed ad libitum do not chew their food as thoroughly as their wild relatives.

Shift in diets can have an immediate impact on structures such as the mandible, due to bone remodeling (Anderson et al., 2014; Kiliaridis, 2006) or on teeth with permanent eruption such as the incisors, due to modulation of their growth rate (Renaud et al., 2019). By contrast, murine molars are characterized by a finite growth and are only affected by wear after eruption; they are therefore not prone to plastic variation along life. However, the present results show that shifts in diet, as those observed in sub-Antarctic mice switching from an omnivorous to more carnivorous behavior (van Aarde & Jackson, 2007; Le Roux et al., 2002), might get an immediate and measurable geometric signature on the molar geometry, due to differences in wear trajectories. This opens perspectives to characterize short-terms variations in diet in wild populations and even in the fossil record, but a limitation will be to estimate a proxy of age. Weight appeared here as a convincing proxy to trace advancing use, and it is routinely available for wild-trapped animals, but it may exhibit between-populations differences due to nutrition and health conditions (Renaud, Hardouin, et al., 2017). Body length may avoid such drawbacks, but it can still vary due to local conditions, for instance in insular contexts (Lomolino, 2005). Mandible size could be measured even on museum specimens for which body size was not collected, but it appeared here to poorly trace wear trajectories. The problem will be even more difficult for fossil teeth found isolated.

5.3 | A complex three-dimensional pattern of occlusion

Our results further showed that the geometric changes of the molar row occurring as age increases as a function of diet-related

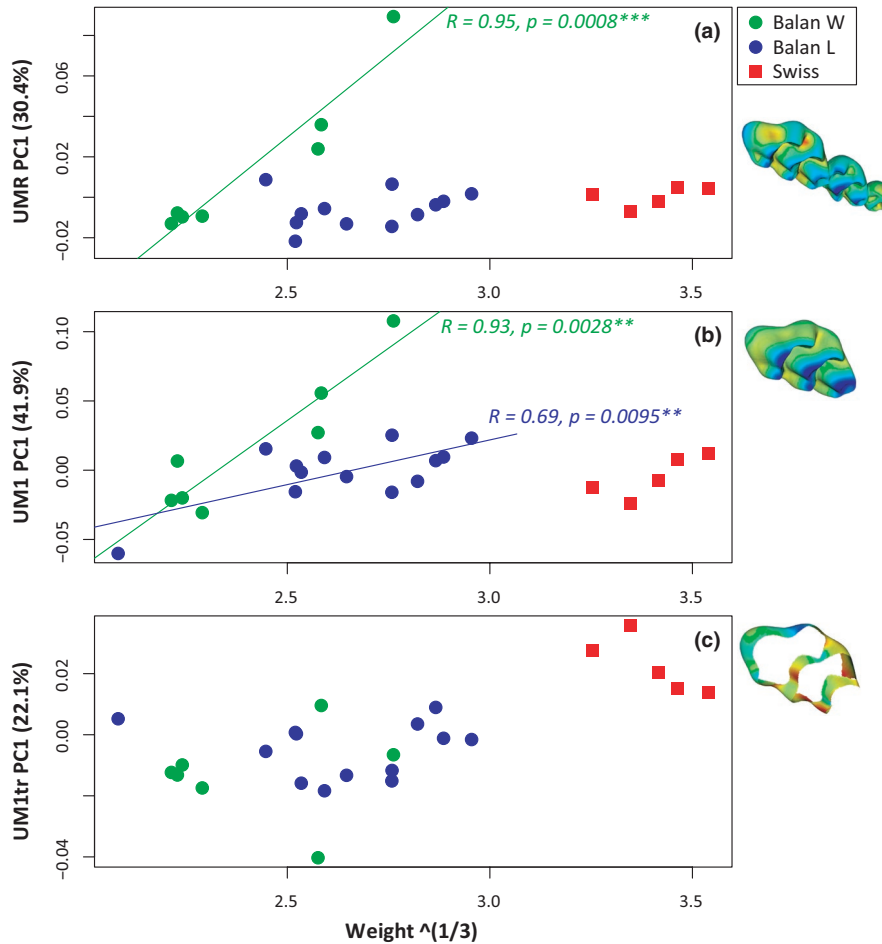


FIGURE 5 Variation of molar shape with weight (cubic root). Shape is represented by scores on PC1. (a) Upper molar row. (b) First upper molar. (c) Truncated first upper molar. Next to each graph, visualization of the deformation from minimum to maximum scores along PC1. In blue compression and in red expansion. Significant associations are represented with regression lines (green, Balan W; blue, Balan L). Swiss mice (in red) are represented but not included in the regressions

masticatory demand did not merely involve wear strictly speaking, but also the alignment of the three molars. Murine rodents are reported to grind food by sliding molar teeth from back to front, according to a propalinal movement (Lazzari et al., 2008). Being bracketed by two longitudinal rows on the lower molar, the median row of cusps is of primary functional importance and, accordingly, it is characterized by a longitudinal alignment of cusps constituting a guide to occlusion in unworn teeth (Figure 9, PC1min). This longitudinal alignment, however, is perturbed in wild-trapped mice. In molar rows characterized by an advanced wear, the second and third molar slightly form an angle with the first upper molar, pointing inwards the mouth (Figure 9, PC1max). Even in relatively unworn molar rows, the third molar is not aligned with the first two molars and it is slightly diverted toward the lingual side (Figure 9, PC2 max).

Analysis of the jaw motion during mastication shows that the closing movement consists of an arched, forward trajectory and that only the late closing phase occurs parallel to the sagittal plane (Utsumi et al., 2010). In wild and lab mice, little worn molar rows seem to display more elevated lingual cusps that may accommodate the lateral component of the lower jaw coming into occlusion from a

slightly labial, posterior direction. With wear, this unbalanced height between the lingual and lateral cusps seems to be levelled out. By contrast, wild and lab mice differ consistently by the alignment of the third molar with the rest of the row.

The upper molar row is inserted at a slight angle from the sagittal plane, the posterior end pointing labially. The third molar erupts around weaning, a time when presumably, the young mice had already incorporated a significant amount of adult food in their diet. The consistent difference observed in the alignment of the molars between wild and lab-bred mice sharing the same genetic background suggests that mechanical loadings related to the consumption of demanding food influence the eruption of the third molar and its position in the jaw, pushing it away into a more lingual position. The insertion of the molars seems to be further modified later on due to a pivoting of the first molar relative to the second one, suggesting a response to high loadings pushing the second molar into the first. Previous results have shown that the jaw system respond to the demand of chewing hard food by a remodeling of the lower jaw bone leading to increased insertion area for the masseter muscles (Anderson et al., 2014). The present results further show that bone

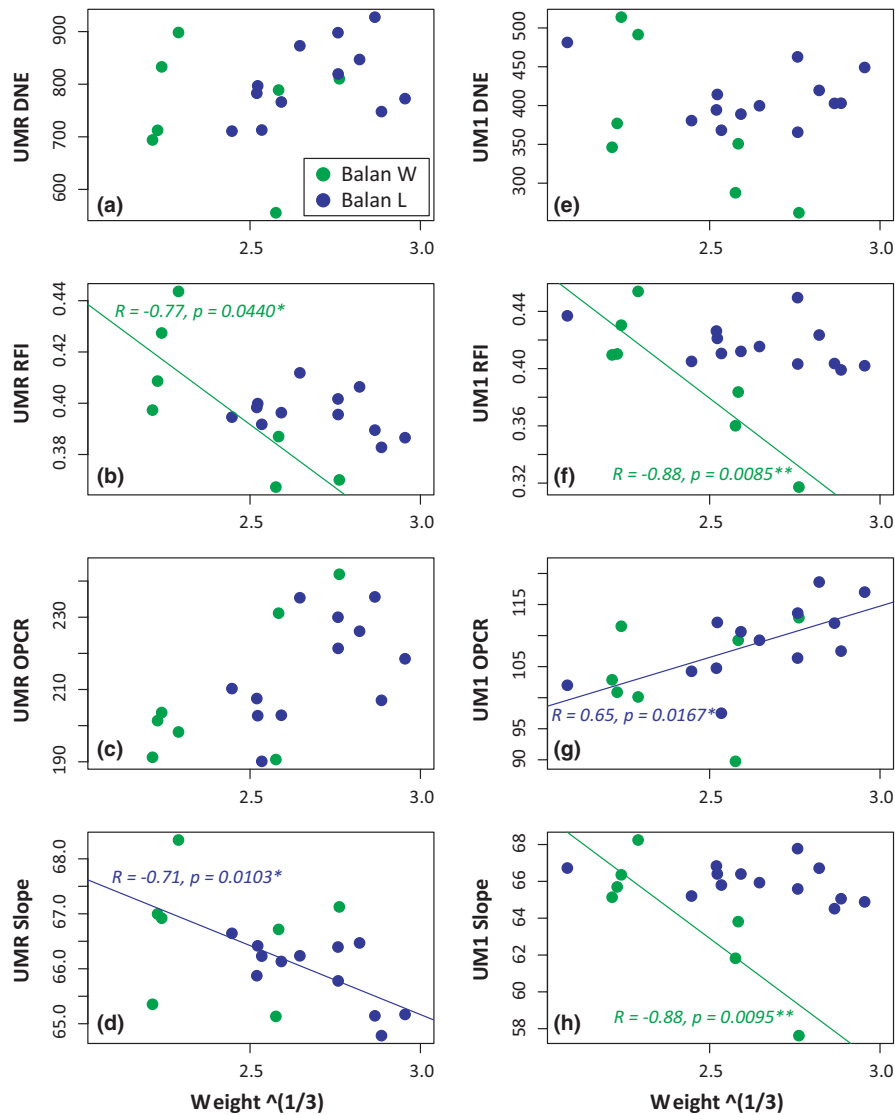


FIGURE 6 Variation of molar topographic parameters with weight (cubic root) for the upper molar row (a–d) and of the first upper molar (e–h) in the two Balan groups (Balan W and Balan L). (a, e) tooth curvature (DNE, Dirichlet Normal Energy). (b, f): tooth relief (RFI, Relief Index). (c, g) tooth complexity (OPCR, Orientation Patch Count Rotated). (d, h) tooth slope. Significant associations are represented with regression lines (green, Balan W; blue, Balan L)

remodeling is involved in accommodating the effect of mechanical loadings on the insertion of the molars. The geometry of the molar row, including the relative position of the teeth, could thus be indicative of diet differences on very short time scales, due to bone plasticity and wear; in that respect, it could be even more informative than considering the first upper molar alone, only affected by wear.

5.4 | Molar topography as a further insight into wear signature

Considering the geometry of the whole molar row appears to provide insights into the impact of the mechanical loadings related to mastication. Because of this very process, however, the occlusal surface of the row is far from being planar. As a consequence, topographic

estimates derived from the whole molar row appear to be more unstable than those estimated on the first molar row only. This molar, including its wear facets, seems to retain only traces of the late close phase, occurring along the sagittal plane (Lazzari et al., 2008).

Topographic parameters estimated from the tooth surface capture functionally relevant properties, such as sharpness and complexity, which may vary with dietary specialization across species (Godfrey et al., 2012; Ungar, 2004). Herbivorous species tend to display higher molar complexity than carnivores (Evans et al., 2007) because many facets help crushing food items (Winchester et al., 2014). By contrast, carnivores tend to possess molars with sharp cusps for puncturing and shearing tendons, muscles, or insect cuticles. A high relief may constitute a resistance to abrasive diet (Evans et al., 2007). Within species, however, these topographical parameters appear to mostly vary with wear (Pampush, Spradley, et al., 2016;

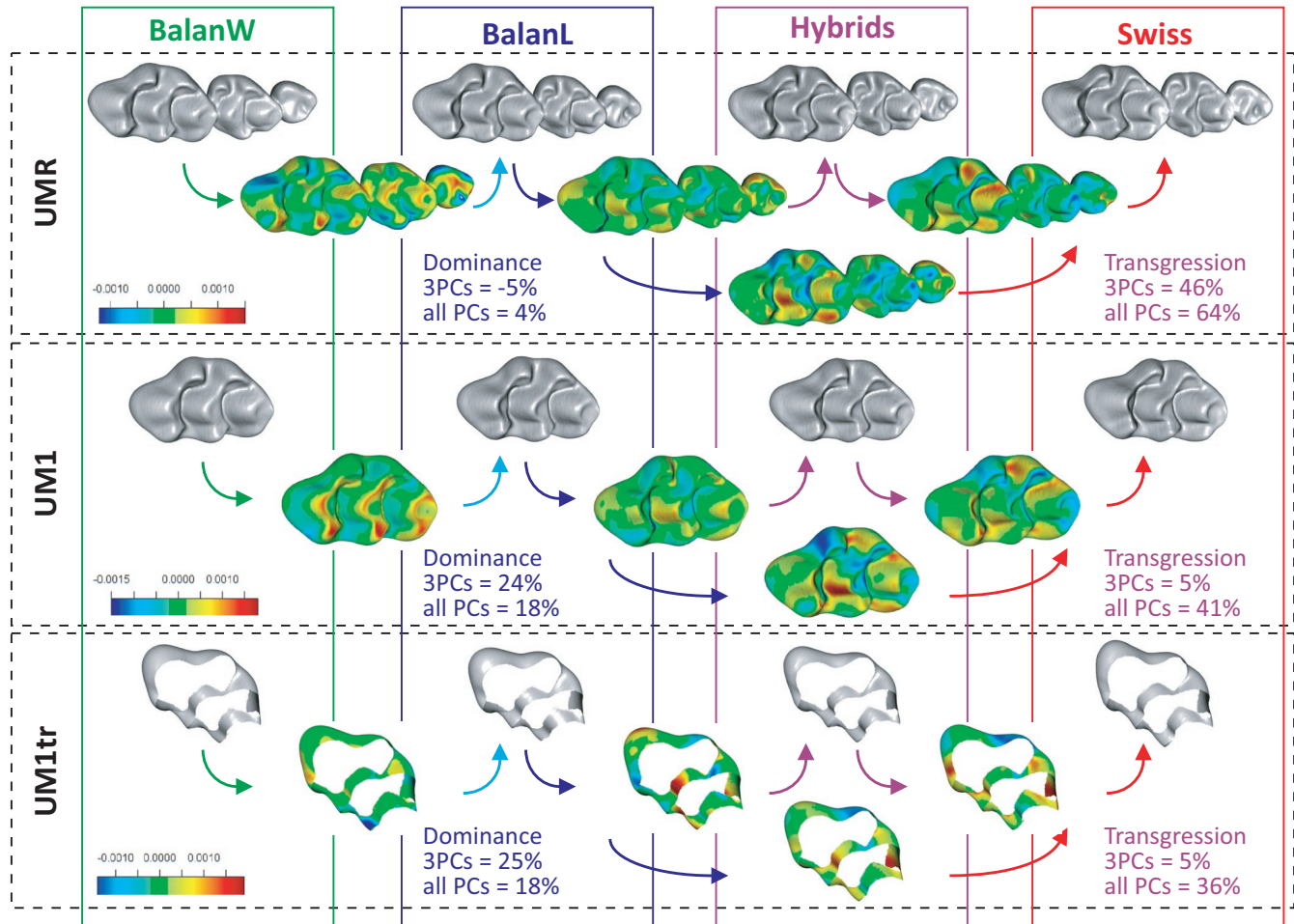


FIGURE 7 Shape differences between groups, and effects of hybridization between Balan laboratory offspring and Swiss mice. Group mean shapes are depicted from left to right (grey meshes); from top to bottom, the three molar descriptors. Colored meshes represent the change from one mean shape to another. Blue areas indicate compression and red expansion; all meshes to the same color scale for a given molar descriptor. Dominance and transgression value characterizing hybrids are given

TABLE 4 Differences in tooth geometry and topography between lab-bred offspring of wild mice (Balan L) and Swiss mice. Differences in shape between the two groups were tested using a multivariate analysis of variance (ffmanova) on the first three PC axes; differences in univariate parameters using t-tests. *p*-values are provided; in bold: *p* < 0.001; underlined: *p* < 0.01; in italics: *p* < 0.05

		UMR	UM1	UM1tr
Shape	PC1-PC3 (ffmanova)	2.29e-06	9.05e-07	1.125e-06
Size	Centroid Size	0.0001	0.2838	0.6306
Topography	DNE	0.2375	<u>0.0081</u>	
	RFI	0.4008	0.0166	
	OPCR	<u>0.0064</u>	1.437e-05	
	Slope	0.1114	<u>0.0022</u>	

Renaud & Ledevin, 2017; Renaud et al., 2018). The present results confirm the important effect of wear on topographic parameters. Relief and slope are of course the most strongly associated with wear, since relief describes the abrasion of the tooth, and slope is necessarily decreased when the cusps become flattened. As a consequence, the variation of these parameters is more important within wild-trapped mice. Sharpness (DNE) varies as well through age, but contrary to monkeys (Pampush, Spradley, et al., 2016), it

shows a progressive decrease because cusp tips become blunted, an effect that is not counterbalanced in murine rodents by the development of new edges. By contrast, the mouse dentition maintains its complexity with age (Renaud & Ledevin, 2017) and even seems here to increase with advancing wear, possibly corresponding to a case of “molar sculpting,” when molar morphology can sustain and even increase functional performance through wear (Pampush, Spradley, et al., 2016). The quantification of topographic parameters at the

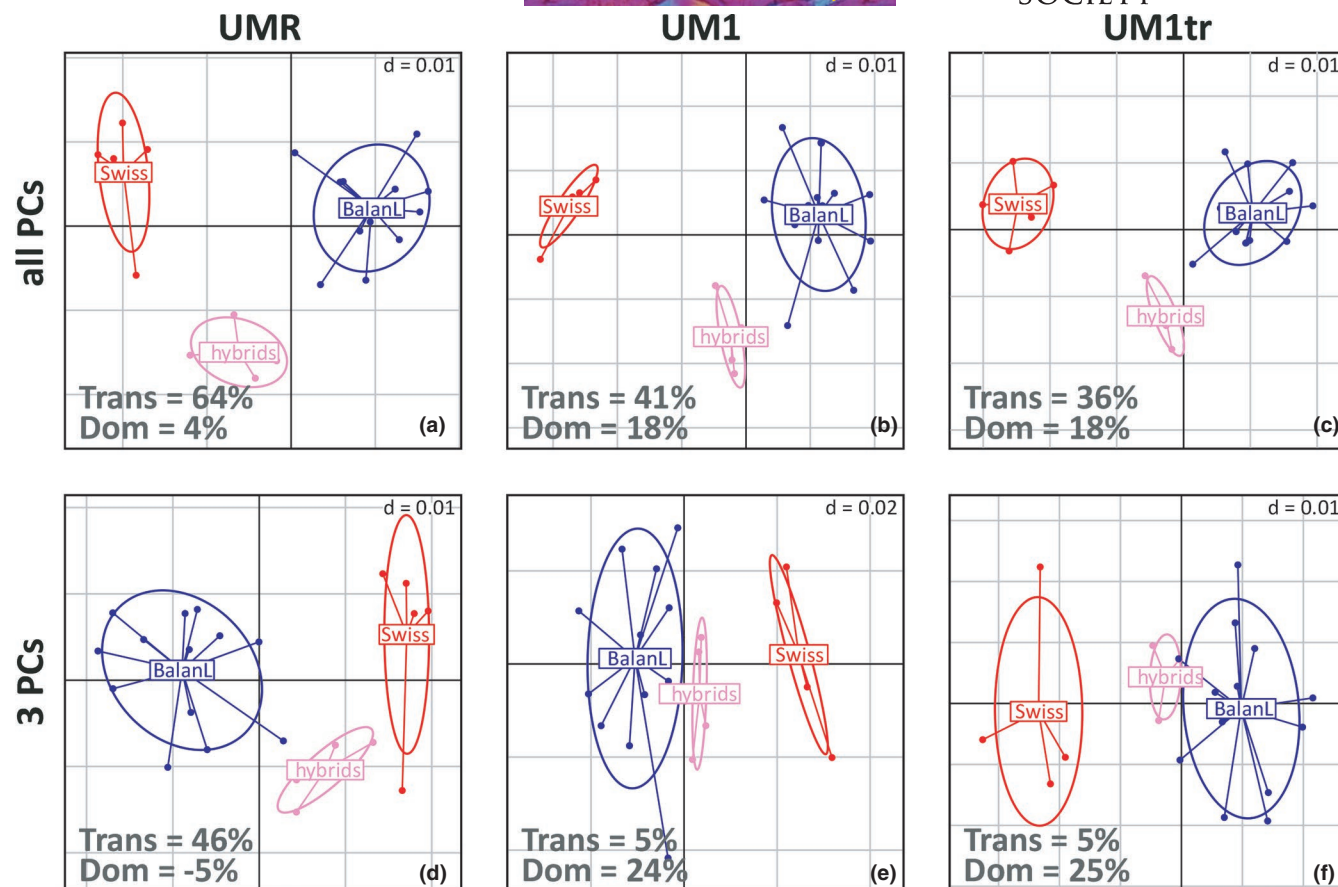


FIGURE 8 Molar shape differentiation between Balan and Swiss mice, and their hybrids. The first two axes of a between-group principal component analysis (bgPCA) on all axes of the PCA (a–c) and on the first three axes of the PCA (d–f) are shown. (a, d) UMR. (b, e) UM1. (c, f) truncated UM1. The size of the grid is indicated on the upper right of each graph. “Trans” indicates the percentage of transgression of the hybrids relative to the inter-parent distance. “Dom” indicates the percentage of dominance; positive value corresponds to a dominance of the wild parent (Balan L)

intra-specific scale may thus shed further light on the dynamics of wear as a function of age and occlusal demand. A wide dispersion of relief, sharpness, and slope indices within a population, as exemplified in the wild-trapped mice, may point to a high abrasive demand strongly flattening and blunting cusps along the animals' life.

5.5 | Morphological differences between wild mice and lab strain

Among the classical mouse strains, the Swiss strain is the closest to *M. m. domesticus* (Yang et al., 2011). Derived in the early 20th century, it is characterized by a very large body size since it weighted twice as much as Balan mice considered here. By contrast, the first upper molar did not differ in size between the wild and Swiss mice. This discrepancy between body and molar size may appear surprising because molar size is considered as a good proxy of the animal size, but this relationship is valid at a broad taxonomic scale (Gingerich et al., 1982) and not necessarily at an intraspecific level, as shown by comparisons among house mouse populations (Renaud, Hardouin, et al., 2017). This is due to the fact that the size of the first upper molar is

determined during prenatal growth, and is not necessarily impacted by large body size achieved during postnatal growth. However, if the first upper molar was of similar size in wild and Swiss mice, the upper molar row as a whole was significantly larger in Swiss mice. The size of the molar row also includes the second and especially the third molar, which erupts at weaning. Larger body size of Swiss mice may let more space for the late developing molars, explaining the discrepancy between the molar row and the first molar.

The Swiss mice also differ from the wild ones in their molar geometry. The Swiss strain differs from wild mice by details, such as its more pronounced posterior labial cusp (t9), and by characteristics that seem to affect the longitudinal alignment of median row of cusps (Figure 9): the central cusp of the UM1 (t5) is slightly expanded labially whereas the anterior part of the tooth point inwards (lingually). Such shape changes may appear functionally unfavorable by disrupting the postero-anterior guide to the lower jaw movement. Nevertheless, this geometry corresponded to a higher complexity index than in wild mice, although higher complexity is generally considered of adaptive value. Possibly, given the slight torsion of the molar row, the change in the orientation of the t5 does not deeply affect the alignment of the cusps and is not maladaptive (Figure 9). Alternatively, since the

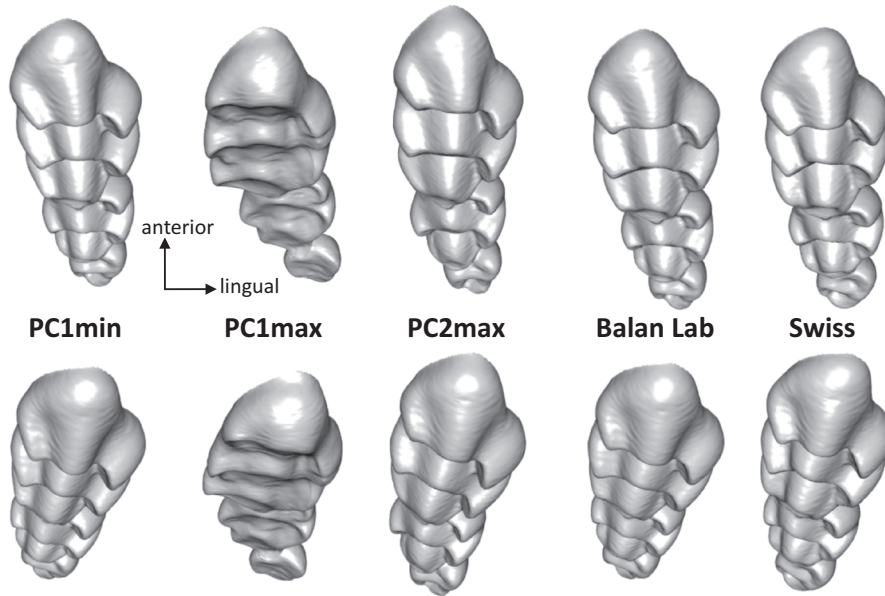


FIGURE 9 Comparison of upper molar row morphologies. From left to right: molar rows displaying little and advanced wear, summarized by minimum and maximum scores respectively on PC1 (see Figure 5a); molar row corresponding to young wild mice (PC2max); molar row mean shape in lab offspring of wild mice and in Swiss mice. Above: view of the molar row along its main axis; below: molar row closer to its functioning position, with the insertion on the jaw close to horizontal and the posterior side slightly diverted labially

Swiss strain evolved in a context of captivity with food ad libitum, the relaxation of the mastication demand may also have allowed unfavorable morphological changes to evolve. This suggests that small dental changes involved in most intra-specific variation, which may occur due to inbreeding in small populations functioning as demes (Pocock et al., 2004) or in strains as in the case of the Swiss mice, can lead to a small increase in complexity but that their interpretation in terms of functional advantage should be cautious (Renaud et al., 2018).

5.6 | Morphological signature of hybridization

Beyond their difference in body size, Swiss and wild-derived mice thus appear to be characterized by molar size and shape differences. Their offspring displayed a mosaic response to hybridization, with an intermediate body mass, as expected for additive effects, but a dominance of the larger Swiss parent for the size of the molar row and a dominance of the wild parent for molar shape, associated with a more or less pronounced transgressive pattern. The molar row consistently displayed the most important transgressive component, whereas transgression was almost fully absent of the first-order shape signal when considering the first molar alone.

Transgressive phenotypes are most often explained as due to the accumulation of genes with antagonistic effects in each parental group, which can produce transgression from the F2 generation onwards (Rieseberg et al., 1999). However, such process cannot explain transgression in F1 hybrids, as those considered here, and epistasis in complex traits is a more likely explanation (Stelkens & Seehausen, 2009). The geometry of the molar row describes both the shape of each molar, and their relative size. It thus includes both a component of dominance toward the wild parental group for the UM1 shape, and a dominance toward the Swiss parent for the relative size of the second and third molars. This combination may alone generate transgressive hybrid phenotypes, as a novel mosaic of features derived

from both parental groups (Renaud et al., 2012). Furthermore, the molar row is known to develop as a cascade, the first molar influencing the development of the subsequent ones (Kavanagh et al., 2007). Epigenetic interactions between molar teeth, and with neighboring tissues, may be more important in late developing molars, leading to higher degrees of transgression; similarly, higher transgression was found in late developing parts of the UM1 (Renaud, Alibert, et al., 2017).

Regarding the first molar itself, dominance toward the wild parental group was found, most pronounced when considering the first shape axes only. Such pattern can be expected if the divergence of the Swiss strain involved the accumulation of recessive alleles and further argues for a morphological evolution due to inbreeding in a context of relaxed selection. Transgression was not present when focusing on the most prominent shape features, but reached ~40% of the parental divergence when considering all components of shape. This complex structure of transgression, weak along the axes expressing the divergence between parental groups but overall relatively high, may echo the finding that in molars of inter-specific hybrids, the most differentiated regions were the less transgressive (Renaud, Alibert, et al., 2017). Hybrids between well-differentiated parents also often appear as intermediate (Savriama et al., 2018), whereas transgression is important in hybrids of poorly differentiated parents (Kozitzky, 2021), in agreement with the general observation that transgression is negatively correlated to the amount of genetic divergence between hybridizing taxa (Stelkens & Seehausen, 2009). This may correspond, at the scale of the tooth, to the fact that most differentiation between Swiss and wild mice involves few genes segregated among the parental groups, displaying dominance toward the wild parent but no transgression. Molar shape determinism is however highly polygenic (Pallares et al., 2017), and epistasis may buffer phenotypic differentiation for many genes, but promotes transgression on these very traits showing no differentiation.

6 | CONCLUSIONS

The analysis of the molar row appeared the most efficient to capture in all its complexity the dental response to use, by quantifying, together with wear strictly speaking, changes in the insertion of the late developing molars due to loading during mastication. Focusing on the first molar still characterized wear patterns and improved the estimates of topographic parameters. The truncated model of the first molar was confirmed as a “wear-free” descriptor that emphasizes differences with a genetic basis. Because of their different sensitivity to the sources of genetic and non-genetic variation, comparing the different descriptors could pinpoint several key features.

Wild-trapped mice and their laboratory offspring displayed important differences ascribed to the effect of mastication on the dentition. Wear, as documented on the first upper molar, appeared to be more pronounced but qualitatively similar in the wild populations compared with lab-bred offspring. By contrast, molar rows of wild and lab-bred mice differed qualitatively because of changes in molar insertion related to loading during mastication. Swiss and wild mice displayed a consistent difference in molar shape pointing to a genetic differentiation despite the relatively recent isolation of the laboratory strain and its phylogenetic closeness to *M. m. domesticus*. This confirms that molar shape can evolve fast in isolation (Chevret et al., 2021), but these differences are of second order compared with the impact of wear on the molar geometry.

Diet changes in wild populations could thus leave a measurable signature on the molar geometry and topography, but because these changes seem to be mostly recognized on the age-related trajectory, they may be difficult to infer in fossil specimens. Wear-effects could anyway generate variation in molar shape and topography that are as or even more important than genetic differences between populations, urging for cautious interpretations of these results when comparing wild populations.

ACKNOWLEDGMENTS

We warmly thank the horse stable Les Peupliers (Balan) for their authorization and support during the trapping. We also thank the anonymous reviewers whose constructive comments contributed to improve the manuscript. We acknowledge the contribution of SFR Biosciences (UMS3444/CNRS, US8/Inserm, ENS de Lyon, UCBL) AniRa-ImmOs facility, and we particularly thank Mathilde Bouchet for her kind assistance during the scanning sessions. This work was supported by the Fédération de Recherche BioEnviS – FR3728 of University Claude Bernard Lyon 1.

CONFLICT OF INTEREST

The authors declare that they have no competing interests.

DATA AVAILABILITY STATEMENT

The 3D models of the molar rows are deposited in MorphoMuseuM. <https://doi.org/10.18563/journal.m3.141>. Data about the scanned specimens, centroid size, PC scores and topographic parameters can be found in Table S1.

ORCID

Yoland Savriama  <https://orcid.org/0000-0002-9980-584X>

Caroline Romestaing  <https://orcid.org/0000-0002-6877-9626>

Ronan Ledevin  <https://orcid.org/0000-0002-1936-9612>

Sabrina Renaud  <https://orcid.org/0000-0002-8730-3113>

REFERENCES

- Adams, C.D. & Otarola-Castillo, E. (2013) geomorph: an R package for the collection and analysis of geometric morphometric shape data. *Methods in Ecology and Evolution*, 4, 393. <https://doi.org/10.1111/2041-210X.12035>
- Anderson, P.S.L., Renaud, S. & Rayfield, E.J. (2014) Adaptive plasticity in the mouse mandible. *BMC Evolutionary Biology*, 14, 85. <https://doi.org/10.1186/1471-2148-14-85>
- Besl, P.J. & McKay, N.D. (1992) A method for registration of 3-D shapes. *IEEE Transactions on Pattern Analysis and Machine Intelligence*, 14, 239–256. <https://doi.org/10.1109/34.121791>
- Bookstein, F.L. (1997) Landmark methods for forms without landmarks: morphometrics of group differences in outline shape. *Medical Image Analysis*, 1, 225–243. [https://doi.org/10.1016/S1361-8415\(97\)85012-8](https://doi.org/10.1016/S1361-8415(97)85012-8)
- Boyer, D.M. (2008) Relief index of second mandibular molars is a correlate of diet among prosimian primates and other euarchontan mammals. *Journal of Human Evolution*, 55, 1118–1137. <https://doi.org/10.1016/j.jhevol.2008.08.002>
- Bunn, J.M., Boyer, D.M., Lipman, Y., Clair, E.M.S., Jernvall, J. & Daubechies, I. (2011) Comparing Dirichlet normal surface energy of tooth crowns, a new technique of molar shape quantification for dietary inference, with previous methods in isolation and in combination. *American Journal of Physical Anthropology*, 145, 247–261. <https://doi.org/10.1002/ajpa.21489>
- Chevret, P., Hautier, L., Ganem, G., Herman, J., Agret, S., Auffray, J.-C. et al. (2021) Genetic structure in Orkney island mice: isolation promotes morphological diversification. *Heredity*, 126, 266–278. <https://doi.org/10.1038/s41437-020-00368-8>
- Cignoni, P., Callieri, M., Corsini, M., Dellepiane, M., Ganovelli, F. & Ranzuglia, G. (2008) MeshLab: an open-source mesh processing tool. *Sixth Eurographics Italian Chapter Conference*, 129–136. <https://doi.org/10.2312/LocalChapterEvents/ItalChap/ItalianChapConf2008/129-136>
- de Winter, J.C.F. (2013) Using the Student's t-test with extremely small sample sizes. *Practical Assessment, Research and Evaluation*, 18, 1–12.
- Evans, A.R. & Jernvall, J. (2009) Patterns and constraints in carnivoran and rodent dental complexity and tooth size. *Journal of Vertebrate Paleontology*, 29, 92A. SVP Program and Abstracts Book.
- Evans, A.R., Wilson, G.P., Fortelius, M. & Jernvall, J. (2007) High-level similarity of dentitions in carnivorans and rodents. *Nature*, 445, 78–81. <https://doi.org/10.1038/nature05433>
- Firmat, C., Gomes Rodrigues, H., Renaud, S., Claude, J., Hutterer, R., Garcia-Talavera, F. et al. (2010) Mandible morphology, dental microwear, and diet of the extinct giant rats *Canariomys* (Rodentia: Murinae) of the Canary Islands (Spain). *Biological Journal of the Linnean Society*, 101, 28–40. <https://doi.org/10.1111/j.1095-8312.2010.01488.x>
- Gingerich, P.D., Smith, B.H. & Rosenberg, K. (1982) Allometric scaling in the dentition of primates and prediction of body weight from tooth size in fossils. *American Journal of Physical Anthropology*, 58, 81–100. <https://doi.org/10.1002/ajpa.1330580110>
- Godfrey, L.R., Winchester, J.M., King, S.J., Boyer, D.M. & Jernvall, J. (2012) Dental topography indicates ecological contraction of lemur communities. *American Journal of Physical Anthropology*, 148, 215–227. <https://doi.org/10.1002/ajpa.21615>

- Grossnickle, D.M., Smith, S.M. & Wilson, G.P. (2019) Untangling the multiple ecological radiations of early mammals. *Trends in Ecology & Evolution*, 34, 936–949. <https://doi.org/10.1016/j.tree.2019.05.008>
- Hayden, L., Lochovska, L., Sémon, M., Renaud, S., Delignette-Muller, M.-L., Vicot, M. et al. (2020) Developmental variability channels mouse molar evolution. *eLife*, 9, e50103. <https://doi.org/10.7554/eLife.50103>
- Hunter, J.P. & Jernvall, J. (1995) The hypocone as a key innovation in mammalian evolution. *Proceedings of the National Academy of Sciences of the United States of America*, 92(23), 10718–10722. <https://doi.org/10.1073/pnas.92.23.10718>
- Kavanagh, K.D., Evans, A.R. & Jernvall, J. (2007) Predicting evolutionary patterns of mammalian teeth from development. *Nature*, 449, 427–432. <https://doi.org/10.1038/nature06153>
- Kiliaridis, S. (2006) The importance of masticatory muscle function in dentofacial growth. *Seminars in Orthodontics*, 12, 110–119. <https://doi.org/10.1053/j.sodo.2006.01.004>
- Kozitzky, E.A. (2021) The Impact of hybridization on upper first molar shape in robust Capuchins (*Sapajus nigritus* × *S. libidinosus*). *Dental Anthropology*, 32, 13–34. <https://doi.org/10.26575/daj.v34i1.316>
- Langsrud, Ø. & Mevik, B.-H. (2012) fmanova: fifty-fifty MANOVA. <https://CRAN.R-project.org/package=fmanova>
- Lazzari, V., Tafforeau, P., Aguilar, J.-P. & Michaux, J. (2008) Topographic maps applied to comparative molar morphology: the case of murine and cricetine dental plans (Rodentia, Muroidea). *Paleobiology*, 34, 46–64. <https://doi.org/10.1666/06052.1>
- Le Roux, V., Chapuis, J.-L., Frenot, Y. & Vernon, P. (2002) Diet of the house mouse (*Mus musculus*) on Guillou Island, Kerguelen archipelago, Subantarctic. *Polar Biology*, 25, 49–57. <https://doi.org/10.1007/s003000100310>
- Ledevin, R., Chevret, P., Ganem, G., Britton-Davidian, J., Hardouin, E.A., Chapuis, J.-L. et al. (2016) Phylogeny and adaptation shape the teeth of insular mice. *Proceedings of the Royal Society of London, Biological Sciences (Series B)*, 283, 20152820. <https://doi.org/10.1098/rspb.2015.2820>
- Lomolino, M.V. (2005) Body size evolution in insular vertebrates: generality of the island rule. *Journal of Biogeography*, 32, 1683–1699. <https://doi.org/10.1111/j.1365-2699.2005.01314.x>
- López-Antoñanzas, R., Renaud, S., Peláez-Campomanes, P., Azar, D., Kachacha, G. & Knoll, F. (2019) First levantine fossil murines shed new light on the earliest intercontinental dispersal of mice. *Scientific Reports*, 9, 11874. <https://doi.org/10.1038/s41598-019-47894-y>
- Misonne, X. (1969) *African and Indo-Australian Muridae*. *Evolutionary trends*. Musée Royal de l'Afrique Centrale.
- Pallares, L.F., Ledevin, R., Pantalacci, S., Turner, L.M., Steingrimsson, E. & Renaud, S. (2017) Genomic regions controlling shape variation in the first upper molar of the house mouse. *eLife*, 6. <https://doi.org/10.7554/eLife.29510>
- Pampush, J.D., Spradley, J.P., Morse, P.E., Griffith, D., Gladman, J.T., Gonzales, L.A. et al. (2018) Adaptive wear-based changes in dental topography associated with atelid (Mammalia: Primates) diets. *Biological Journal of the Linnean Society*, 124, 584–606. <https://doi.org/10.1093/biolinnean/bly069>
- Pampush, J.D., Spradley, J.P., Morse, P.E., Harrington, A.R., Allen, K.L., Boyer, D.M. et al. (2016) Wear and its effects on dental topography measures in howling monkeys (*Alouatta palliata*). *American Journal of Physical Anthropology*, 161(4), 705–721. <https://doi.org/10.1002/ajpa.23077>
- Pampush, J.D., Winchester, J.M., Morse, P.E., Vining, A.Q., Boyer, D.M. & Kay, R.F. (2016) Introducing molaR: a new R package for quantitative topographic analysis of teeth (and other topographic surfaces). *Journal of Mammalian Evolution*, 23(4), 397–412. <https://doi.org/10.1007/s10914-016-9326-0>
- Pocock, M.J.O., Searle, J.B. & White, P.C.L. (2004) Adaptations of animals to commensal habitats: population dynamics of house mice *Mus musculus domesticus* on farms. *Journal of Animal Ecology*, 73, 878–888. <https://doi.org/10.1111/j.0021-8790.2004.00863.x>
- R Core Team. (2018) *R: a language for environment and statistical computing*. R Foundation for Statistical Computing.
- Renaud, S., Alibert, P. & Auffray, J.-C. (2012) Modularity as a source of new morphological variation in the mandible of hybrid mice. *BMC Evolutionary Biology*, 12, 141. <https://doi.org/10.1186/1471-2148-12-141>
- Renaud, S., Alibert, P. & Auffray, J.-C. (2017) Impact of hybridization on shape, variation and covariation of the mouse molar. *Evolutionary Biology*, 44, 69–81. <https://doi.org/10.1007/s11692-016-9391-6>
- Renaud, S., Delépine, C., Ledevin, R., Pisanu, B., Quéré, J.-P. & Hardouin, E.A. (2019) A sharp incisor tool for predator house mice back to the wild. *Journal of Zoological Systematics and Evolutionary Research*, 57, 989–999. <https://doi.org/10.1111/jzs.12292>
- Renaud, S., Hardouin, E.A., Quéré, J.-P. & Chevret, P. (2017) Morphometric variations at an ecological scale: seasonal and local variations in feral and commensal house mice. *Mammalian Biology*, 87, 1–12. <https://doi.org/10.1016/j.mambio.2017.04.004>
- Renaud, S. & Ledevin, R. (2017) Impact of wear and diet on molar row geometry and topography in the house mouse. *Archives of Oral Biology*, 81, 31–40. <https://doi.org/10.1016/j.archoralbio.2017.04.028>
- Renaud, S., Ledevin, R., Souquet, L., Gomes Rodrigues, H., Ginot, S., Agret, S. et al. (2018) Evolving teeth within a stable masticatory apparatus in Orkney mice. *Evolutionary Biology*, 45, 405–424. <https://doi.org/10.1007/s11692-018-9459-6>
- Renaud, S., Pantalacci, S. & Auffray, J.-C. (2011) Differential evolvability along lines of least resistance of upper and lower molars in island house mice. *PLoS One*, 6, e18951. <https://doi.org/10.1371/journal.pone.0018951>
- Renaud, S., Romestaing, C. & Savriama, Y. (2021) 3D models related to the publication: wild versus lab house mice: effects of age, diet, and genetics on molar geometry and topography. *MorphoMuseum*, 7, e141. <https://doi.org/10.18563/journal.m3.141>
- Rieseberg, L.H., Archer, M.A. & Wayne, R.K. (1999) Transgressive segregation, adaptation and speciation. *Heredity*, 83, 363–372. <https://doi.org/10.1038/sj.hdy.6886170>
- Savriama, Y., Valtonen, M., Kammonen, J.I., Rastas, P., Smolander, O.-P., Lyyski, A. et al. (2018) Bracketing phenogenotypic limits of mammalian hybridization. *Royal Society Open Science*, 5, 180903. <https://doi.org/10.1098/rsos.180903>
- Schlager, S. (2015) Meshing operations on triangular meshes. Available from: <https://github.com/zarquon42b/mesheR> [Accessed 28th July 2021].
- Schlager, S. (2017) Chapter 9. Morpho and Rvcg – shape analysis in R: R-packages for geometric morphometrics, shape analysis and surface manipulations. In Zheng, G., Li, S. & Székely, G. (Eds.). *Statistical shape and deformation analysis* (pp. 217–256). Academic Press.
- Skinner, M.M. & Gunz, P. (2010) The presence of accessory cusps in chimpanzee lower molars is consistent with a patterning cascade model of development. *Journal of Anatomy*, 217, 245–253. <https://doi.org/10.1111/j.1469-7580.2010.01265.x>
- Slice, D., Bookstein, F.L., Marcus, L. & Rohlf, F.J. (1996) Appendix I. A glossary for geometric morphometrics. *NATO ASI Serie A: Life Sciences*, 284, 531–552.
- Stelkens, R. & Seehausen, O. (2009) Genetic distance between species predicts novel trait expression in their hybrids. *Evolution*, 63, 884–897. <https://doi.org/10.1111/j.1558-5646.2008.00599.x>
- Thioulouse, J., Dray, S., Dufour, A.-B., Siberchicot, A., Jombart, T. & Pavoine, S. (2018) *Multivariate analysis of ecological data with ade4*. Springer.
- Ungar, P. (2004) Dental topography and diets of *Australopithecus afarensis* and early *Homo*. *Journal of Human Evolution*, 46, 605–622. <https://doi.org/10.1016/j.jhevol.2004.03.004>
- Utsumi, D., Nakamura, A., Matsuo, K., Zeredo, J.L., Koga, Y. & Yoshida, N. (2010) Motor coordination of masseter and temporalis muscle during mastication in mice. *International Journal of Stomatology and Occlusion Medicine*, 3, 187–194. <https://doi.org/10.1007/s12548-011-0068-6>

- Valenzuela-Lamas, S., Baylac, M., Cucchi, T. & Vigne, J.-D. (2011) House mouse dispersal in Iron Age Spain: a geometric morphometrics appraisal. *Biological Journal of the Linnean Society*, 102, 483–497. <https://doi.org/10.1111/j.1095-8312.2010.01603.x>
- van Aarde, R.J. & Jackson, T.P. (2007) Food, reproduction and survival in mice on sub-Antarctic Marion Island. *Polar Biology*, 30, 503–511. <https://doi.org/10.1007/s00300-006-0209-3>
- Wade, C.M., Kulbokas III, E.J., Kirby, A.W., Zody, M.C., Mullikin, J.C., Lander, E.S. et al. (2002) The mosaic structure of variation in the laboratory mouse genome. *Nature*, 420, 574–578. <https://doi.org/10.1038/nature01252>
- Wiley, D.F., Amenta, N., Alcantara, D.A., Deboshmita, G., Kil, Y.J., Delson, E. et al. (2005) *Evolutionary morphing*. IEEE Visualization. IEEE.
- Winchester, J.M., Boyer, D.M., St. Clair, E.M., Gosselin-Ildari, A.D., Cooke, S.B. & Ledogar, J.A. (2014) Dental topography of platyrrhines and prosimians: convergence and contrasts. *American Journal of Physical Anthropology*, 153, 29–44. <https://doi.org/10.1002/ajpa.22398>
- Yang, H., Wang, J.R., Didion, J.P., Buus, R.J., Bell, T.A., Welsh, C.E. et al. (2011) Subspecific origin and haplotype diversity in the laboratory mouse. *Nature Genetics*, 43, 648–655. <https://doi.org/10.1038/ng.847>
- Zuccotti, L.F., Williamson, M.D., Limp, W.F. & Ungar, P.S. (1998) Technical note: modeling primate occlusal topography using geographic information systems technology. *American Journal of Physical Anthropology*, 107, 137–142. [https://doi.org/10.1002/\(SICI\)1096-8644\(199809\)107:1<137:AID-AJPA11>3.0.CO;2-1](https://doi.org/10.1002/(SICI)1096-8644(199809)107:1<137:AID-AJPA11>3.0.CO;2-1)

SUPPORTING INFORMATION

Additional supporting information may be found online in the Supporting Information section.

How to cite this article: Savriama, Y., Romestaing, C., Clair, A., Averty, L., Ulmann, J., Ledevin, R. & et al (2022) Wild versus lab house mice: Effects of age, diet, and genetics on molar geometry and topography. *Journal of Anatomy*, 240, 66–83. <https://doi.org/10.1111/joa.13529>